function of the size of these alkyl substituents: smaller substituents should be able to pass one another readily[30] than should large ones. Hence, increasing the alkyl group size on the epoxide should lead to an *increase* in stereospecificity, provided that this increase in alkyl group size did not adversely affect the rate of ring closure. Clearly, reducing congestion about the metal (bigger ionic size, smaller ligands) would enhance this cyclization rate.

**Acknowledgment.** The authors acknowledge generous support for this work by the National Science Foundation (Grant No. CHE-79-00996). Y.H. thanks Mitsubishi Petrochemical Company (Japan) for financial support.

(30) For example, see: Doering, W. von E.; Barsa, E. A. *Tetrahedron Lett.* **1978**, 2495 and references cited therein.

**Registry No.** *cis*-2,3-Dimethyloxirane, 1758-33-4; *trans*-2,3-dimethyloxirane, 21490-63-1; *cis*-2,3-epoxy-4-methylpentane, 3204-02-2; *trans*-2,3-epoxy-4-methylpentane, 2390-95-6; *cis*-2,3-dipropyloxirane, 1439-06-1; *trans*-2,3-dipropyloxirane, 1689-70-9; 7-oxabicyclo[4.1.0]heptane, 286-20-4; 8-oxabicyclo[5.1.0]octane, 286-45-3; ethyloxirane, 106-88-7; *cis*-2-ethyl-3-methyloxirane, 3203-99-4; *trans*-2-ethyl-3-methyloxirane, 3203-98-3; $V(acac)_2$, 14024-62-5; $V(dpm)_2$, 78624-81-4; $V(tfa)_2$, 78624-82-5; $Mo(acac)_2$, 34346-27-5; $Mo(dpm)_2$, 78624-83-6; *cis*-2-butene, 590-18-1; *trans*-2-butene, 624-64-6; *cis*-4-methyl-2-pentene, 691-38-3; *trans*-4-methyl-2-pentene, 674-76-0; *cis*-4-octene, 7642-15-1; *trans*-4-octene, 14850-23-8; cyclohexene, 110-83-8; cycloheptene, 628-92-2; 1-butene, 106-98-9; *cis*-2-pentene, 627-20-3; *trans*-2-pentene, 646-04-8.

**Supplementary Material Available:** A table of deoxygenation of epoxides to olefins (1 page). Ordering information is given on any current masthead page.

Contribution from the Department of Chemistry, Northeastern University, Boston, Massachusetts 02115

# Characterization of the Thermolysis Products of $Fe(TPTZ)_2Cl_2 \cdot nH_2O$ and the Related 2,4,6-Tris(2-pyridyl)-1,3,5-triazine Complexes $Zn(TPTZ)Cl_2$ and $Fe(TPTZ)Cl_3$

DIANA SEDNEY, MINA KAHJEHNASSIRI, and WILLIAM MICHAEL REIFF*

*Received February 4, 1981*

A new five-coordinate ferrous complex, $Fe(TPTZ)Cl_2$, has been synthesized. The neat powder form of this species undergoes a slow, irreversible oxidation in the atmosphere at ambient temperature to the very strongly antiferromagnetically coupled ferric dimer $[Fe(TPTZ)Cl_2]_2O$. These complexes as well as the related $Zn(TPTZ)Cl_2$ and $Fe(TPTZ)Cl_3$ complexes are characterized by a variety of physical methods.

## Introduction

Thermolysis of a series of six-coordinate low-spin bis(terpyridine) ferrous compounds, $Fe(2,2',2''\text{-terpyridine})_2X_2$, produces complexes which are five-coordinate when $X = Br^-$, $I^-$, and $NCS^-$ and high-spin by replacing one neutral tridentate ligand with two monovalent counteranions. The double salt $[Fe(terpy)_2]^{2+}[FeCl_4]^{2-}$ is obtained upon thermolysis of $Fe(terpy)_2Cl_2$.[1] The latter double salt complex contains a very stable low-spin, pseudooctahedral cation and a well-known pseudotetrahedral ferrous anion. Another bis(triimine)iron(II) compound has been thermolized in the present study in an attempt to add a chloride member to this series. Heating the navy blue, low-spin $Fe(2,4,6\text{-tris}(2\text{-pyridyl})\text{-}1,3,5\text{-triazine})_2Cl_2 \cdot nH_2O$ (hereafter, $Fe(TPTZ)_2Cl_2$) does result in a new species, $Fe(TPTZ)Cl_2$. Unlike the mono(terpyridine) complexes, however, this gray blue TPTZ product is air sensitive and upon prolonged exposure to air oxidizes to a green complex, believed to be a $\mu$-oxo dimer.

Zero- and high-field Mössbauer spectroscopy, magnetic susceptibility measurements, IR spectra, and X-ray powder and solution conductivity measurements are presented below as means to identify each of these new species. Schematic diagrams of the tris(pyridyl)triazine and 2,2',2''-terpyridine ligands are shown in Figure 1. The similarity of their tridentate nature is apparent.

## Experimental Section

**Preparation of [Dichloro[bis(2,4,6-tris(2-pyridyl)-1,3,5-triazine)iron Dihydrate.** This compound and its thermolysis products were first prepared by M. Kahjehnassiri.[2] A solution of the TPTZ ligand in absolute ethanol was added to freshly prepared $FeCl_2 \cdot 4H_2O$ in a 2.1:1 ligand to metal ratio. The navy blue salt was precipitated after reducing the volume of the solution to only a few milliliters and subsequently adding acetone. The product was recrystallized from absolute ethanol and acetone.

**Preparation of $Fe(TPTZ)Cl_2$.** The $Fe(TPTZ)_2Cl_2 \cdot 2H_2O$ starting material was placed in a thermolysis oven and heated under vacuum ($\sim 10$ $\mu$m) to 180 °C for $\sim 10$ h. The ligand was observed to come off between 170 and 180 °C, and the final product represented $\sim 60\%$ weight loss. The original sample had turned grayish blue. Gravimetric factors for the calculation of the theoretical yield of the bis-to-mono conversion are in the range of 0.5843–0.5577 with the assumption of zero to two waters of hydration in the precursor. Anal. Calcd for $FeC_{18}H_{12}N_6Cl_2$: C, 49.16; H, 2.73; N, 19.12. Found: C 49.06; H, 2.87; N, 19.29.[2]

**Preparation of $[Fe(TPTZ)Cl_2]_2O \cdot 2H_2O$.** After exposure to air for several months, the *gray-blue* polycrystalline $Fe(TPTZ)Cl_2$ sample converts to a *light green* material. Prolonged vacuum thermolysis of this new material at $T \approx 200$ °C had no effect, suggesting that the gray-blue to green conversion does not involve a readily reversible *oxygenation*. The progression of the conversion was monitored by Mössbauer spectroscopy. Spectral parameters and susceptibility results (to be discussed) show that the conversion involves *oxidation* of the ferrous centers. Anal. Calcd for $[Fe(TPTZ)Cl_2]_2O \cdot 2H_2O$: C, 46.42; H, 2.99; N, 18.05; Fe, 12.03. Found: C, 46.33; H, 2.46; N, 17.72; Fe, 12.4.

**Preparation of $Fe(TPTZ)Cl_3 \cdot 1.5H_2O$.** In this preparation, a methanol solution of the ligand (2.56 mM) was added to a methanol solution of nominally anhydrous $FeCl_3$ (1.28 mM) under gaseous nitrogen. The yellowish orange product was filtered under vacuum and washed with absolute methanol twice. Anal. Calcd for $[Fe(TPTZ)Cl_3]_2 \cdot 3/2H_2O$: C, 43.00; H, 2.99; N, 16.74. Found: C, 43.26; H, 2.53; N, 16.81.

(1) W. M. Reiff, W. A. Baker, and N. E. Erickson, *Inorg. Chem.*, **8**, 2019 (1969).

(2) M. Kahjejnassiri, Master Degree Thesis, Northeastern University, 1974.

0020-1669/81/1320-3476$01.25/0 

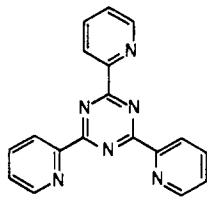

*2, 4, 6 - tripyridyl - s - triazine (TPTZ)*

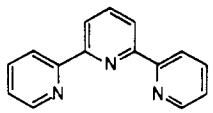

*2, 2', 2" - terpyridine (terpy)*

**Figure 1.** Schematic diagrams of the triimine ligands 2,2',2''-terpyridine and 2,4,6-tris(pyridyl)-1,3,5-triazine.

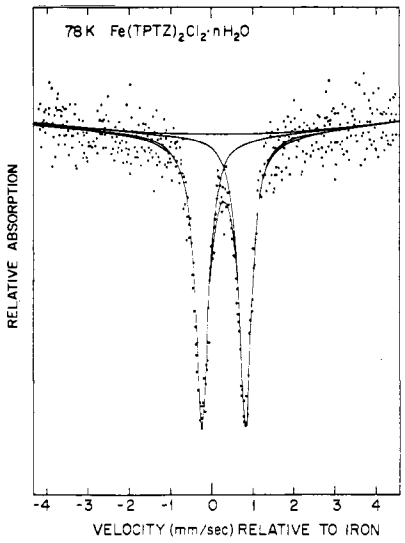


**Figure 2.** Mössbauer spectrum of $[Fe(TPTZ)_2Cl_2] \cdot nH_2O$ at 78 K including least-squares Lorentzian fit.

**Preparation of $Zn(TPTZ)Cl_2$.** A ligand to metal molar ratio of 1:1 was used. An absolute ethanol solution of the ligand (1.6 mM) was added to an absolute ethanol solution of $ZnCl_2$. The yellowish white precipitate of $[Zn(TPTZ)Cl_2]$ was immediately formed. The crystals were filtered, washed with absolute ethanol four times, and then dried in an vacuum desiccator. Anal. Calcd for $Zn(TPTZ)Cl_2$: C, 48.18; H, 2.67; N, 18.73. Found: C, 48.09; H, 2.86; N, 18.71.

**Microanalysis.** Microanalyses for carbon, hydrogen, nitrogen, and iron were performed by Chemalytics, Inc., Tempe, AZ 85281, and Galbraith Laboratories, Knoxville, TN 37921.

**Physical Measurements. Magnetic Susceptibility Measurements.** The initial susceptibility data were determined on a standard Gouy apparatus. More detailed low-temperature measurements were made with the use of a Faraday balance including a Cahn electrobalance, a Varian 4-in. electromagnet (field varying from 1.6 to 5.1 kG), and a Janis Super Vari-Temp cryostat. Temperature measurement and control were based on calibrated silicon and uncalibrated gallium arsenide diodes, respectively. Temperatures below 4.2 K were determined with the use of both a calibrated silicon diode and helium vapor-pressure thermometry.

**Zero-field iron-57 Mössbauer spectroscopy measurements** were made with use of a conventional constant acceleration spectrometer and a Janis Super Vari-Temp cryostat with temperature measurements via a calibrated silicon diode. High-field Mössbauer spectra at 4.2 K were obtained with the use of a superconducting niobium–tin solenoid.

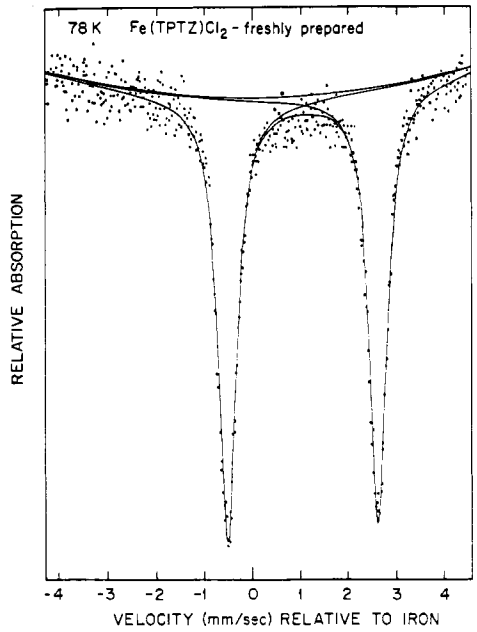


**Figure 3.** Mössbauer spectrum of $[Fe(TPTZ)Cl_2]$ at 78 K including least-squares Lorentzian fit.

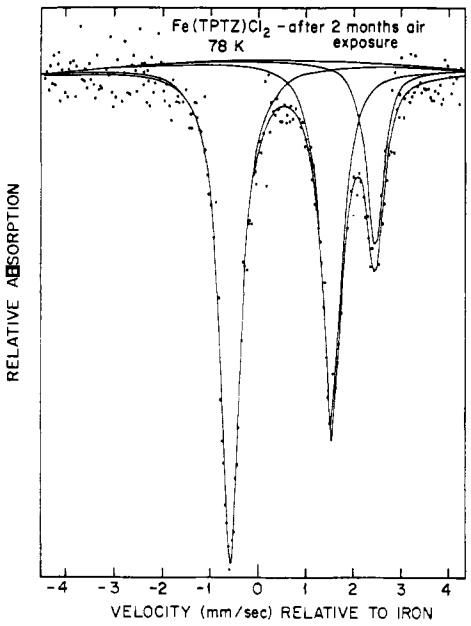


**Figure 4.** Mössbauer spectrum (78 K) of $[Fe(TPTZ)Cl_2]$ after exposure to the atmosphere for 2.5 months including least-squares Lorentzian fit.

**X-ray powder patterns** were obtained with copper K$\alpha$ radiation filtered by nickel metal foil. A General Electric camera in conjunction with a General Electric X.R.D.-6 X-ray diffraction unit was used.

**Conductivity measurements** were carried out with the use of a standard Beckman Instruments, Inc., conductivity bridge, Model RC 16B2, with a standard platinum electrode cell and 0.001 M solutions in all cases.

**Visible and near-infrared spectra** were obtained with a Cary Model 14 spectrophotometer. All spectral measurements were made at room temperature. The samples were fluorinated hydrocarbon mulls.

**Infrared absorption spectra** were obtained with a Beckman IR-10 infrared spectrophotometer. The samples were in the form of KBr disks (0.7–1.2 mg of sample per 200–300 mg of KBr) and Nujol mulls. Polyethylene plates were used as the optics for the mulls.

## Results and Discussion

**Zero-Field Mössbauer Spectroscopy.** Mössbauer spectroscopy proves to be a useful technique in monitoring the ap-

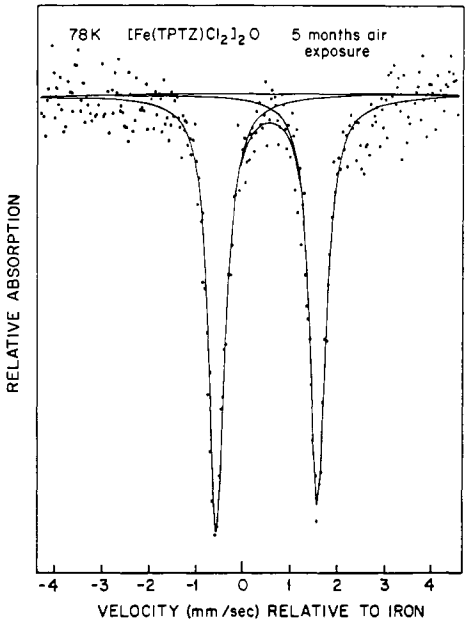


**Figure 5.** Mössbauer spectrum (78 K) of $[Fe(TPTZ)Cl_2]$ after exposure to the atmosphere for ~5 months including least-squares Lorentzian fit.

Table I. Mössbauer Spectra Parameters

| compd | $T$ | $\delta$,[a] mm/s | $\Delta E_Q$, mm/s | spin and oxidation state |
|---|---|---|---|---|
| $Fe(TPTZ)_2Cl_2 \cdot nH_2O$ | 300 | 0.22 | 1.03 | $S = 0$, $Fe^{II}$ |
| | 78 | 0.29 | 1.06 | |
| $Fe(TPTZ)Cl_2$ | 300 | 0.92 | 2.31 | $S = 2$, $Fe^{II}$ |
| | 195 | 0.98 | 2.71 | |
| | 78 | 1.07 | 3.13 | |
| | 4.2 | 1.07 | 3.25 | |
| $[Fe(TPTZ)Cl_2]_2O \cdot 2H_2O$ | 78 | 0.49 | 1.88 | $S = 5/2$, $Fe^{III}$ |
| | 56.5 | 0.47 | 1.88 | |
| | 30 | 0.47 | 1.88 | |
| | 12 | 0.48 | 1.87 | |
| | 4.2 | 0.49 | 1.87 | |
| $Fe(TPTZ)Cl_3$ | 78 | 0.46 | 0.97 | $S = 5/2$, $Fe^{III}$ |

[a] Relative to iron foil.

pearance of new species, during the thermolysis of $Fe(TPTZ)_2Cl_2 \cdot nH_2O$ as evidenced in Figures 2–5. These figures are all spectra determined at 78 K, beginning with the "bis" precursor. Table I lists the Mössbauer spectra parameters for each of these figures as well as for spectra at other temperatures. The isomer shift ($\delta$) and quadrupole splitting ($\Delta E_Q$) of Figure 2 are characteristic of low-spin ferrous complexes and an $^1A$ ground term. This assignment is consistent with the room-temperature magnetic moment (1.44 $\mu_B$) reported by Kahjehnassiri.[2]

After thermolysis, $Fe(TPTZ)_2Cl_2$ is completely converted to a new gray blue species (identified here as compound Q) as demonstrated in Figure 3. Here $\delta$ clearly corresponds to a high-spin iron(II) product. The $\delta$ and $\Delta E_Q$ are reminiscent[1] of the five-coordinate ferrous terpyridine complexes, i.e., a large electric field gradient and an ambient temperature isomer shift ~0.9 mm/s. The latter is *intermediate* to those normally observed for pseudotetrahedral ferrous ($FeN_2Cl_2$) chromophores and pseudooctahedral ($FeN_2Cl_4$) centers with imine nitrogen coordination. A five-coordinate structure is indicated for compound Q, consistent with its elemental analysis and implied formula. If this product is exposed to the air, oxidation occurs slowly in the neat powder. Figure 4 presents the spectrum of the same thermolyzed sample used for Figure 3 after a 2-month air-exposure interval. A second quadrupole doublet is now observed whose low-energy peak overlaps that of compound Q. This oxidized species is designated as compound R. After another 2.5 months had elapsed, oxidation of the sample is nearly complete (see Figure 5).

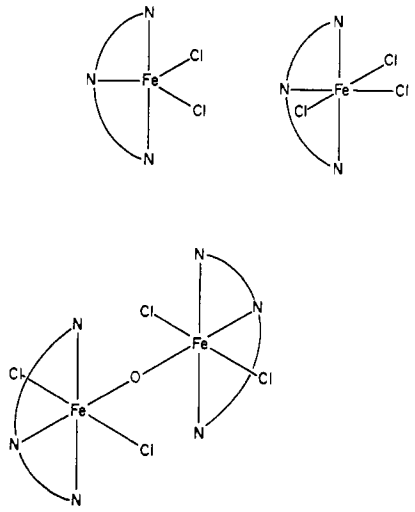

**Figure 6.** Proposed structures for $[Fe(TPTZ)Cl_2]$, $[Fe(TPTZ)Cl_3]$, and $[Fe(TPTZ)Cl_2]_2O$.

Compound R appears to be a ferric, oxo-bridged dimer for which a probable structure is shown in Figure 6. Oxo-bridged dimers are well-known in the literature, but their preparation usually involves a solution synthesis[3] in contrast to the novel solid-state oxidation observed herein. An isomer shift (78 K) of ~0.50 mm/s is typical of these dimers. The Schiff base complex oxobis[(*N*,*N*'-ethylenebis(salicylideniminato))iron] (usually abbreviated as $[Fe(salen)]_2O$, a well-characterized oxo-bridged dimer,[4] has $\delta$ = 0.56 mm/s at 78 K. The $\Delta E_Q$ of 2.16 mm/s (at 78 K) is in the same range noted for oxo-bridged diimine systems (e.g., for $[(Fe(1,10\text{-phen})_2Cl)_2O]Cl_2 \cdot 5H_2O$, $\Delta E_Q$ = 1.68 mm/s at 78 K). Only one triimine oxo-bridged iron(III) dimer has been reported in the literature, $[(Fe(terpy))_2O](NO_3)_4 \cdot H_2O$, and the quadrupole splitting of this complex is even larger ($\Delta E_Q$ = 2.43 mm/s at 78 K).[5,6] The foregoing quadrupole splittings are quite large for high-spin iron(III). The individual iron atoms of the binuclear unit possesses a $^6A$ ground term for which the valence contribution to the electric field gradient tensor is 0. The large electric field gradient is believed to arise from double-bond chracter of the metal–oxygen bridge bonds[7] which apparently leads to a sizable "lattice" contribution to the electric field gradient tensor as discussed subsequently.

**Infrared Spectra.** The infrared spectra of compounds Q and R provide further evidence for the identities of these species. The band occurring at 814 $cm^{-1}$ in compound R's spectrum is assigned as the asymmetric Fe–O–Fe stretch and is one of the chracteristics of oxo-bridged ferric dimers.[3] An oxo- rather than peroxo- or dioxygen formulation is proposed for compound R since no new bands occur in the 1080–1150-$cm^{-1}$ region characteristic of the O–O stretch.[8] In the metal–halogen stretch region of the infrared spectrum of compound R, a band appears at 333 $cm^{-1}$ which is not present in the "bis" precursor or compound Q. This is most likely the $Fe^{III}$–Cl

(3) K. S. Murray, *Coord. Chem. Rev.*, **12**, 1 (1974).
(4) J. Lewis, F. E. Mabbs, and A Richards, *J. Chem. Soc. A*, 1014 (1967).
(5) W. M. Reiff, W. A. Baker, Jr., and N. E. Erickson, *J. Am. Chem. Soc.*, **90**, 4794 (1968).
(6) W. M. Reiff, G. J. Long, and W. A. Baker, Jr., *J. Am. Chem. Soc.*, **90**, 6347 (1968).
(7) W. M. Reiff, *J. Chem. Phys.*, **54**, 4718 (1971).
(8) J. P. Collman, J. I. Brauman, T. R. Halbert, and K. S. Suslick, *Proc. Natl. Acad. Sci U.S.A.*, **73**, 3333 (1976).

Table II. Molar Conductivity Data[a]

| compd | ΛM, $\Omega^{-1}$ cm$^2$ mol$^{-1}$ in nitrobenzene | ΛM, $\Omega^{-1}$ cm$^2$ mol$^{-1}$ in nitromethane |
|---|---|---|
| $(CH_3CH_2CH_2CH_2)_4NI$ | 29.85 | 88.12 |
| $[Fe(TPTZ)Cl_2]$ | 6.27 | |
| $[Fe(TPTZ)Cl_3]$ | 3.35 | |
| $[Fe(bpy)_3](ClO_4)_2$ | 59.50 | |
| $[Fe(TPTZ)_2]Cl_2$ | | 161.75 |
| $[Fe(TPTZ)_2]I_2$ | 52.45 | |
| $[Fe(TPTZ)_2](ClO_4)_2$ | 57.78 | |
| $[Zn(TPTZ)Cl_2]$ | | 14.31 |

[a] All solutions are $\sim 10^{-3}$ M.

stretch. For the free ligand, a band appears around 288 cm$^{-1}$. This is greatly increased in intensity in Q's spectrum suggesting that the $Fe^{II}$–Cl stretch overlaps the band. One would expect to see this band shifted to lower energy in compound Q's spectrum corresponding to a lower oxidation number.

**X-ray Measurements.** X-ray powder pattern spectra of the two complexes $[Fe(TPTZ)Cl_2]$ and $[Zn(TPTZ)_2]$ were obtained. From a previous single-crystal X-ray study[9-11] it has been found that $[Zn(terpy)Cl_2]$ has a geometry intermediate between trigonal bipyramidal and square pyramidal. Bis(terpyridine) complexes of $ZnCl_2$ could not be synthesized, indicating the remarkable stability of the five-coordinate species with this metal salt. Using the same analogy, one would expect to obtain a five-coordinate complex by adding a solution of $ZnCl_2$ to a ligand such as TPTZ rather than $[Zn(TPTZ)_2]^{2+}$. The X-ray powder pattern spectra of the two complexes $[Fe(TPTZ)Cl_2]$ and $[Zn(TPTZ)Cl_2]$ are identical. This indicates that these two compounds are isomorphous. By analogy to $Zn(terpy)Cl_2$ and the isomorphism of $Zn(TPTZ)Cl_2$ and $Fe(TPTZ)Cl_2$, the latter complex can be considered as having a geometry intermediate between trigonal bipyramidal and square pyramidal (Figure 6).

**Conductivity Data.** The equivalent conductivity data of a number of complexes obtained in nitrobenzene and nitromethane are summarized in Table II. The conductivities of these solvents were considered to be negligible. A 1:1 electrolyte such as tetrabutylammonium iodide $[(CH_3CH_2CH_2CH_2)_4]NI$ was used as standard. Its molar conductance in nitrobenzene was found to be 29.85 $\Omega^{-1}$ cm$^2$mol$^{-1}$. The two complexes $[Fe(TPTZ)Cl_2]$ and $[Fe(TPTZ)Cl_3]$ had very low conductivities relative to the standard. This indicates the existence of these complexes as neutral species in nitrobenzene. Although the complex $[Fe(TPTZ)Cl_2]$ is undoubtedly a neutral species, extensive disproportionation to $[Fe(TPTZ)_2]^{2+}$ can be observed by color change to intense blue and increase in its conductance with time. The complex $[Zn(TPTZ)Cl_2]$, which is isomorphous to $[Fe(TPTZ)Cl_2]$, also shows a low conductance (14.31 $\Omega^{-1}$ cm$^2$ mol$^{-1}$) relative to the standard in nitromethane (88.12 $\Omega^{-1}$ cm$^2$ mol$^{-1}$) solution. This is also reasonable for a nonelectrolyte species. For comparison to the bis(TPTZ) complexes, the known 1:2 electrolyte $[Fe(bpy)_3](ClO_4)_2$ was selected and gave a molar conductivity of 59.50 $\Omega^{-1}$ cm$^2$ mol$^{-1}$ in nitrobenzene. The conductivities of $[Fe(TPTZ)_2]I_2$ and $[Fe(TPTZ)_2](ClO_4)_2$ are comparable to that for the bipyridine compound and confirm their 1:2 electrolyte nature. The low conductance of $[Fe(TPTZ)Cl_3]$ indicates the coordination of three chloride ions and therefore probable six coordination, i.e., a pseudooctahedral monomer (Figure 6).

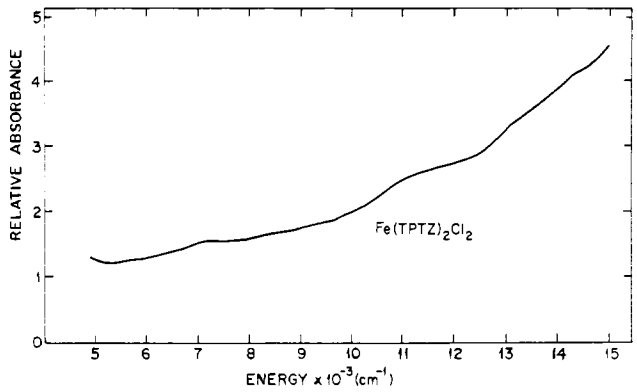


**Figure 7.** Near-infrared–visible spectrum of $[Fe(TPTZ)_2Cl_2] \cdot nH_2O$ (Kel-F mull).

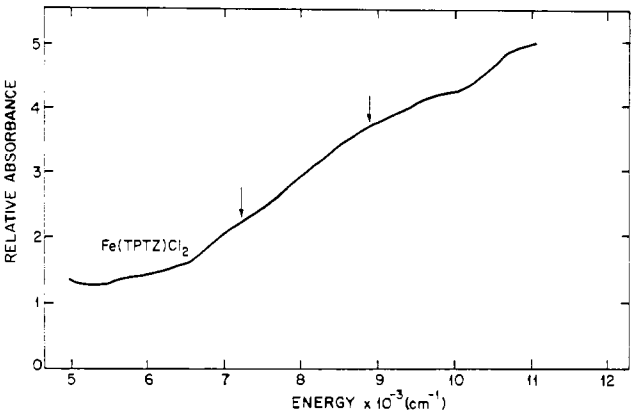


**Figure 8.** Near-infrared–visible spectrum of $[Fe(TPTZ)Cl_2]$ (Kel-F mull).

**Electronic Spectra.** Additional characterization of the spin state and stereochemistry of $[Fe(TPTZ)Cl_2]$ and its precursor $[Fe(TPTZ)_2Cl_2]$ comes from solid-state (mull spectra shown in Figures 7 and 8.. The navy blue low-spin Fe(II) precursor exhibits a series of intense absorptions from the visible well into the UV. These are attributed to the expected combination of $^1A \rightarrow$ (nominal $^1T$, $^1E$) ligand field and $t_{2g}$ (metal) $\rightarrow \pi^*$ (ligand) charge-transfer transitions typical of low-spin ferrous complexes with delocalizing ligands having empty antibonding $\pi$ orbitals. On the other hand, the gray-blue, mono-TPTZ, thermolysis product shows intense, broad absorptions in the range 7000–12 000 cm$^{-1}$ (see arrows in the figure) on a charge-transfer background. The latter are components of the one electron ($^5T_{2g} \rightarrow {}^5E_g$) transition of $O_h$ that is split in the low symmetry of the present $FeN_3Cl_2$ chromophore. While idealized five-coordination corresponds to either $C_{4v}$ or $D_{3h}$ symmetry, the preceding chromophore can have, at most, $C_{2v}$ local symmetry. In this point group, the foregoing single-electron transition of $O_h$ splits into at least three spin-allowed transitions that typically extend from the near-infrared into the visible. The broad band pattern for $[Fe(TPTZ)Cl_2]$ in Figure 7 undoubtedly has its origin in this effect. Unfortunately, it has not proven possible to measure the intensities of these transitions in terms of the extinction coefficients for solution spectra owing to problems of limited solubility and the disproportionation $2[Fe(TPTZ)Cl_2] \rightarrow Fe(TPTZ)_2^{2+} + Fe^{2+} + 4Cl^-$. In any event, the observed near-infrared–visible mull spectrum (albeit broad and poorly resolved) is precisely that expected[1,11] for a distorted, highspin Fe(II) chromophore of five-coordination.

**Magnetic Susceptibility and High-Field Mössbuaer Spectroscopy Results.** Some sample moment data for $Fe(TPTZ)Cl_2$ and its oxidation decomposition product are given in Table III. The precursor $[Fe(TPTZ)_2Cl_2]$ exhibits an

(9) F. W. B. Einstein and B. R. Penfold, *Acta Crystallogr.*, **20**, 924 (1966).
(10) D. E. C. Corbridge and E. G. Cox, *J. Chem. Soc.*, 594 (1966).
(11) J. S. Judge, W. M. Reiff, G. M. Intille, P. Ballway, and W. A. Baker, *J. Inorg. Nucl. Chem.*, **29**, 1711 (1967).

Table III. Experimental Magnetic Moments at Selected Temperatures for Fe(TPTZ)$Cl_2$ and $[Fe(TPTZ)Cl_2]_2O \cdot 2H_2O$

| T, K | $\mu_{eff}$, $\mu_B$ | T, K | $\mu_{eff}$, $\mu_B$ |
|---|---|---|---|
| | Fe(TPTZ)$Cl_2$ | | |
| 304 | 5.10 | 75 | 4.87 |
| 248 | 5.10 | 69 | 4.88 |
| 210 | 5.02 | 63 | 4.90 |
| 189 | 5.00 | 60 | 4.87 |
| 127 | 4.97 | 56 | 4.87 |
| 95 | 4.93 | | |
| | $[Fe(TPTZ)Cl_2]_2O \cdot 2H_2O$ | | |
| 300 | 1.65 | 16.8 | 0.79 |
| 247 | 1.56 | 12.9 | 0.76 |
| 188 | 1.37 | 9.5 | 0.73 |
| 90 | 1.01 | 7.6 | 0.71 |
| 69 | 0.95 | 6.2 | 0.69 |
| 52 | 0.95 | 4.2 | 0.65 |
| 44 | 0.97 | 3.7 | 0.64 |
| 35 | 0.85 | 3.2 | 0.62 |
| 32 | 0.84 | 2.9 | 0.61 |
| 29 | 0.83 | 2.5 | 0.59 |
| 24 | 0.82 | 2.0 | 0.57 |
| 19.3 | 0.81 | 1.7 | 0.55 |

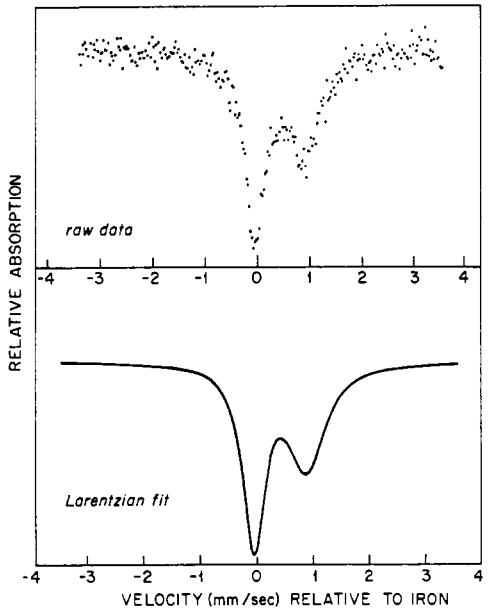


**Figure 9.** Mössbauer spectrum of $[Fe(TPTZ)Cl_3]$ at 78 K.

essentially temperature-independent magnetic moment of ~1 $\mu_B$ expected for low-spin ferrous corresponding to a $^1A$ ground state and is not considered further herein. The six-coordinate ferric monomer Fe(TPTZ)$Cl_3$ also has the expected moment, ~6 $\mu_B$, at ambient temperature. The Mössbauer spectrum of Fe(TPTZ)$Cl_3$ (Figure 9) is also typical of a ferric *monomer* having a small electric field gradient at the metal site. For such monomers, there is often asymmetric broadening of the usual quadrupole doublet owing to slow paramagnetic relaxation.[12] This occurs when there is sufficient separation of metal clusters (≥~7 Å) such that slow spin-spin relaxation results for one or more of three Kramers doublets comprising the $S = {}^5/_2$ sextet state. The slowly relaxing ($m_s = \pm{}^3/_2$ or $\pm{}^5/_2$) doublets arise from the zero-field splitting of the latter sextet.

The initial thermolysis product, Fe(TPTZ)$Cl_2$, is clearly high-spin Fe(II) with an ambient-temperature moment near the spin-only value for $S = 2$, i.e., $24^{1/2}$. This reflects little residual orbital contribution (relative to $O_h$) to $\mu$, consistent

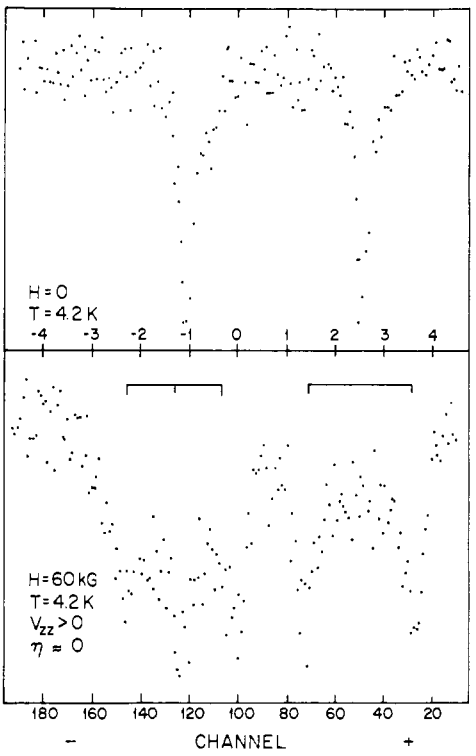


**Figure 10.** Mössbauer spectrum of $[Fe(TPTZ)Cl_2]$ at 4.2 K: $H_{applied}$ = 0 (top); $H_{applied}$ = 50 kG (bottom).

with a distorted five-coordinate environment whose ground term is either $^5A$ or $^5B$. Orbital singlet ground states such as the foregoing lead to large limiting low-temperature values for the quadrupole splitting, as observed (Table I). However, the temperature dependence of the quadrupole splitting for Fe(TPTZ)$Cl_2$ is significant (~1 mm/s over the range 300–4.2 K), suggesting excited orbital states within ~500 $cm^{-1}$ of a ground singlet. Although the magnetic moment is relatively temperature independent down to ~50 K, it is expected to decrease significantly below the spin only value at $T <$ ~20 K owing to zero-field splitting.[13] The analogous five-coordinate ferrous terpyridine complexes ($[Fe(terpy)X_2]$; X = $Br^-$, $I^-$, $NCS^-$) have moments approaching ~3 $\mu_B$ at 2 K owing to this effect.[14] Further studies of the low-temperature magnetic behavior of Fe(TPTZ)$Cl_2$ are planned. Suffice it to say, for now, that we have determined the field dependence of its Mössbauer spectra for 0–60 kG at 4.2 K. The quadrupole interaction is *positive* and axially symmetric (Figure 10). More important in the present context is the fact that no unusual hyperfine splitting effects were observed in the preceding spectra; i.e., the compound behaves as a rapidly relaxing paramagnet with $H_{effective} = H_{applied}$, where $H_{effective} = H_{applied} + H_{internal}$. The absence of an internal hyperfine field suggests a nonmagnetic ($m_s = 0$) single-ion ground state at very low temperatures and positive ($D > 0$) zero-field splitting; i.e., the $^5A$ or $^5B$ are zero-field split such that the $m_s = \pm 2$ Kramers doublet is highest in energy.

While the isomer shift of the Mössbauer spectrum of $[Fe(TPTZ)Cl_2]_2O$ clearly corresponds to *high-spin* iron(III), the ambient-temperature magnetic moment is considerably less than that normally expected for $S = {}^5/_2$ ($35^{1/2} \approx 5.92$ $\mu_B$) and indicates very strong antiferromagnetic exchange. This is further evidenced in the steady decrease in the moment with decreasing temperature (Table III). By comparison with other oxo-bridged ferric dimers, $J$, the intramolecular antiferro-

(12) J. W. G. Wignall, *J. Chem. Phys.*, **44**, 2462 (1966).

(13) K. D. Hodges, R. G. Wollmann, E. K. Barefield, and D. N. Hendrickson, *Inorg. Chem.*, **16**, 2746 (1977).

(14) D. Sedney and W. M. Reiff, to be submitted for publication.

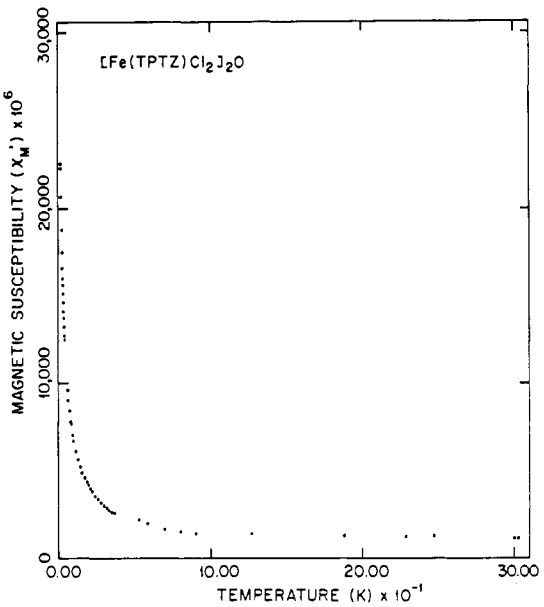


**Figure 11.** Temperature dependence of the molar magnetic susceptibility of $[Fe(TPTZ)Cl_2]_2O$.

magnetic exchange (where $2J$ = the singlet to triplet separation for $S_{TOTAL} = 0$ and $S_{TOTAL} = 1$) is at least $\sim -100$ cm$^{-1}$.[3,7,15] The susceptibility is low and independent of the temperature until below $\sim 50$ K at which it begins to rise (Figure 11). This is attributed to monomeric paramagnetic impurity: in the present case, undoubtedly, the high-spin ferrous precursor $Fe(TPTZ)Cl_2$.

Certain features of the zero- and high-field Mössbauer spectra of $[Fe(TPTZ)Cl_2]O$ are particularly noteworthy and offer additional support of its formulation as an antiferromagnetically coupled, oxo-bridged ferric dimer. First of all, there is the unusally large and temperature-independent quadrupole splitting ($\sim 1.9$ mm/s). The electric field gradient tensor is usually small of 0 for the $^6A$ ground term of high-spin Fe(III) since there is no direct valence-shell-electron contribution for the spherically symmetric, $d^5$ ferric core. Thus, the quadrupole splittings of *simple* ferric monomers are typically in the range 0 to $\sim 1$ mm/s, e.g., the last entry of Table I. The large splitting observed for $[Fe(TPTZ)Cl_2]_2O$ and other oxo-bridged ferric dimer systems is attributed to partial metal–oxygen double-bond character for the bridging bonds. This introduces a large negative principal component ($V_{zz}$) to the electric field gradient tensor and thus a negative quadrupole coupling constant for the case of $^{57}Fe$. The latter are correlated with *stronger*, chemical bonding along a unique molecular axis as opposed to in-plane bonding. We have measured Mössbauer spectra of $[Fe(TPTZ)Cl_2]_2O$ at 4.2 K in longitudinal applied fields of up to 60 kG. These spectra show that (1) $V_{zz}$ is, in fact, *negative* and axial and (2) $H_{effective} = H_{applied}$. As mentioned before, the absence of an internal hyperfine field is correlated with a nonmagnetic ground state. For the present dimer complex, this corresponds to the isolated, total spin ($S_T$) equal 0 ground state resulting from strong antiferromagnetic exchange coupling between equivalent, oxo-bridged ferric centers.

## Conclusions

The spectroscopic and magnetic data presented herein indicate that thermolysis of the low-spin $[Fe(TPTZ)_2]Cl_2$ leads to a five-coordinate iron(II) monomer that undergoes slow oxidation to a binuclear species. This unusual solid-state oxidation was not expected and to our knowledge has no precedent for simple five-coordinate systems. We have found that analogous ferrous terpyridine complexes are stable toward such oxidation. By way of contrast, Martell has prepared some five-coordinate Schiff base iron(II) complexes which form oxo-bridged complexes in solution but are inert to oxidation in the solid state.[16] This aspect of the problem is the subject of future research.

**Acknowledgment.** We wish to acknowledge the support of the National Science Foundation, Division of Materials Research, Solid State Chemistry Program, Grant No. DMR-80 16441.

**Registry No.** $Fe(TPTZ)_2Cl_2$, 78529-70-1; $Fe(TPTZ)Cl_2$, 78529-69-8; $[Fe(TPTZ)Cl_2]_2O$, 78529-68-7; $Fe(TPTZ)Cl_3$, 78529-67-6; $Zn(TPTZ)Cl_2$, 78529-66-5.

(15) C. Chih Ou, R. G. Wollman, D. N. Hendrickson, J. A. Potenza, and H. J. Schugar, *J. Am. Chem. Soc.*, **100**, 4717 (1978).

(16) R. H. Niswander and A. E. Martell, *Inorg. Chem.*, **17**, 1511 (1978).

Contribution from the Department of Chemistry, Northeastern University, Boston, Massachusetts 02115

# Magnetic Susceptibility Study of Bis(diethyldithiocarbamato)manganese(II). A Sulfur-Bridged Linear-Chain Antiferromagnet

GLENN A. EISMAN and WILLIAM MICHAEL REIFF*

The magnetic susceptibility of bis(diethyldithiocarbamato)manganese(II) has been determined from 300 to 2 K for fields varying from 0 to 14 kG. The magnetic moment decreases from $\sim 5.4$ to 0.4 $\mu_B$, and the susceptibility exhibits a broad maximum at $\sim 65$ K. These results are correlated with an intrachain antiferromagnetic exchange, $J/k = -7.5$ K.

## Introduction

In continuing with the study of polymeric transition-metal chains, it was thought that the compound bis(diethyldithiocarbamato)manganese(II), hereafter $Mn(dtc)_2$, could exhibit interesting low-temperature magnetic behavior because of preliminary magnetic work[1] to 84 K that indicated the possibility of antiferromagnetic interactions. The dithiocarbamate ligand, pictured in Figure 1 (top), is an ideal ligand for systematic transition-metal magnetism studies. It not only allows

(1) M. Ciampolini and C. Mengozzi, *J. Chem. Soc., Dalton Trans.*, 2051 (1975).

0020-1669/81/1320-3481$01.25/0 